Evaluation of the effectiveness of the bulk thermal stresses for kraft recovery boiler fireside deposit cleaning

Article *in* Tappi Journal · April 2006

2 authors, including:

Honghi Tran
University of Toronto
221 PUBLICATIONS **1,306** CITATIONS

SEE PROFILE

Evaluation of the effectiveness of the bulk thermal stresses for kraft recovery boiler fireside deposit cleaning

SELÇUK ÖZCAN AND HONGHI TRAN

ABSTRACT: Removal of fireside deposits from the heat transfer tubes in kraft recovery boilers is carried out by sootblowing and occasionally "chill-and-blow" practices. During chill-and-blow, black liquor flow is reduced to rapidly cool the deposits. Thermal stresses generated in the deposit as a result of thermal shock can effectively weaken the deposit, facilitating its cleaning. For this study, we investigated the mechanical weakening effect of thermal stresses generated by the transient temperature gradients. We quantified the mechanical weakening effect due to thermal shock by measuring the decrease in biaxial flexure strength of a preheated sodium chloride disk at various quenching times and surface heat transfer coefficients. We observed that the mechanical weakening occured by transient thermal stresses as well as crack propagation. Approximately 35% loss in biaxial flexure strength could be achieved at heat transfer coefficients above $3.3 \cdot 10^3$ W/m^{2}K, and at quenching durations above 40 s.

Application: The information in this report may help mills more effectively remove fireside deposits from recovery boilers.

The recovery boiler is an essential unit of the kraft pulping process. In the kraft recovery boiler the fouling of the heat exchanger passages by the fireside deposits via the condensation of volatilized inorganic materials (fume), and sticking of carryover particles is counteracted by the continual operation of the sootblowers. Steam blown at typically 1.8 MPa through the nozzles cleans the accumulated deposits by mechanical impact. The effectiveness of these sootblowers depends on the location, frequency of use, and thermal and mechanical properties of the deposits.

Fireside deposits typically consist of 50%-80% sodium sulfate (Na_2SO_4), 10%-40% sodium carbonate (Na_2CO_3), and 1%-15% sodium chloride (NaCl). Deposits may contain as much as 7%-8% potassium salts, and minor amounts of reduced sulfur compounds [1]. Condensed inorganic fume forms a fine dust of submicron size particles. This type of deposition is more significant in the economizer region where the temperature of the flue gas is lower and the flow path is more tortuous than in other regions. The quantity of the fume generated in the lower furnace is in the range of 5%-15% of the sodium that enters the boiler with black liquor.

Carryover particles, on the other hand, are much larger than the dust particles, ranging up to a few millimeters. If the amount of the molten phase contained in the particles is in a certain range, they stick on the tubes upon impact. If the liquid phase is below 15% the adhesion between the carryover and the tube is not sufficient for stickiness, and if the liquid phase is above 70% it flows off the tube surface. The sticky range usually occurs in the superheater. This region is susceptible to fireside deposit fouling by carryover particles. It is estimated that the quantity of carryover is a few percent of the smelt flow [2].

When fouling is more severe than can be coped with by sootblowers, a technique called "chill-and-blow" may be applied. Black liquor flow to the boiler is stopped, and the auxiliary oil guns are activated to decrease the furnace temperature about 300°C in less than 10 min. Subsequently, the sootblowers are activated. The deposits are removed in big chunks, not only during the cooling period, but also during the reheating of the furnace, suggesting that thermal stresses may have an effect in deposit removal.

Martinez [3] proposed thermal stresses generated by transient temperature gradients, interfacial stresses generated by the difference in thermal expansion of the deposit and the steel tube, and tessellated stresses generated by phase transitions. That study found that the minimum temperature difference required to successfully thermally shock elastic deposit-like materials containing a 0.2 mm flaw would be approximately 250°C. The linear thermal expansion coefficient of the fireside deposit was measured to be approximately three times larger than that of carbon steel. These results suggested that thermal stresses induced by transient temperature gradients, and the stresses generated on the steel-deposit interface, might have an effect on deposit removal. Although three of the phase transformations of Na_2SO_4, and Na_2CO_3 were detected, they were accompanied with negligible volume changes, and hence, phase transformations were regarded as ineffective in deposit removal.

Thermal stresses can be calculated for perfectly elastic materials knowing the elastic modulus, linear thermal expansion coefficient, and the temperature distribution, by the theoretical analysis given by Boley and Weiner [4]. Resistance to weakening or fracture of brittle materials subjected to a temperature gradient is termed *thermal shock resistance*, which is governed by two groups of parameters: $\sigma_f/E\alpha$ and k, where σ_f is the fracture strength, E is the elastic modulus, α is the linear thermal expansion coefficient, and k is the thermal conductivity.

Thermal shock resistance increases with increasing fracture strength since it would be necessary to generate a higher stress for failure. It also increases with decreasing elastic modulus, and linear

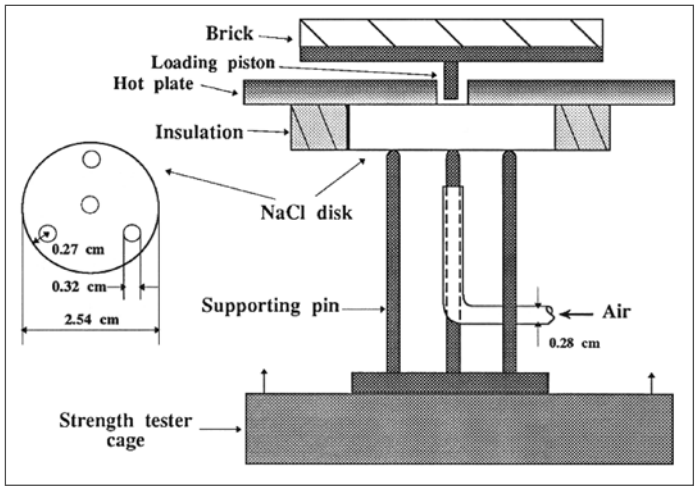

1. Schematic of the biaxial flexure test apparatus.

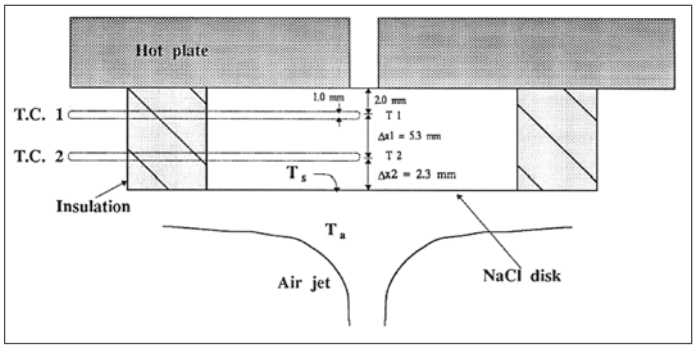

2. Schematic of the apparatus for heat transfer coefficient measurement.

expansion coefficient since for a given temperature difference, strain would be lower, which in turn results in a lower stress. Therefore, materials with higher values of $\sigma_f/E\alpha$ are more resistant to the effects of thermal shock. Thermal conductivity determines the rate of change of temperature distribution inside a body. The final temperature distribution is reached faster, and hence the associated transient stresses vanish more rapidly. Manson and Smith showed how the dimensionless surface stress changes with dimensionless time at various values of Biot modulus for different geometries [5,6].

The maximum normal stress criterion states that when the stress anywhere within the body reaches a certain value of σ_f, failure occurs [5,6]. However, repetitive tests under presumably similar experimental conditions do not yield identical results; the strength also depends on the manner of loading, i.e., tension, bending, torsion etc. The maximum risk of rupture criterion introduced by Weibull's statistical theory successfully explains the phenomenon. The criterion is based on the fact that flaws that exist in any material prevent it from reaching the potential strength in a strength test. Dispersion of flaws in length, density, etc., causes the often observed distribution of test results. Stresses tend to amplify near the flaw tips, increasing the risk of rupture. Therefore, if a body is under uniform stress, the risk of rupture is greater than if only a small region near the surface is subjected to the same stress value, while the rest of the body is under lower stresses.

Thermal stresses can damage a material in a few possible ways. If the stresses are large enough, cracks, especially on the surface, may be initiated. In severe cases, the body may spall and fall apart. In lower thermal stress cases, propagation of pre-existing cracks mechanically weakens the material. Even if thermal stresses are not sufficiently large for crack propagation, they may constitute additional stresses to outside loading, increasing the probability of failure at a lower loading stress. For example, the effect of thermal stresses on a group of firebricks was shown by Goodrich, confirming the mechanical weakening by thermal cycles [7].

The conditions which govern crack propagation were studied by Hasselman [8]. In the worst-case model (i.e. the whole body under the maximum stress), the critical temperature difference required for crack propagation goes through a minimum with increasing crack length. There is a region of crack instability, which is bounded by lower and upper initial crack lengths. The region of crack instability encompasses a wider range of initial crack lengths as the temperature difference increases.

At the critical temperature difference for a given crack length, kinetic crack propagation starts, and the crack length rapidly reaches its subcritical value, with a corresponding abrupt decrease in material strength. For short cracks, after crack initiation the rate of strain energy release exceeds the surface fracture energy and the excess energy appears as the kinetic energy of the propagating crack. When the crack length reaches to the upper limit of instability, it still has kinetic energy and continues to propagate until the total surface fracture energy offsets the total energy released. After the temperature difference reaches a second critical value, the crack restarts to propagate in a quasi-static manner.

EXPERIMENTAL

Evaluation of transient thermal stresses by biaxial flexure test

The effectiveness of thermal stresses generated by transient temperature gradients in the deposit removal process was investigated by measuring the initial strength loss of polycrystalline NaCl disks as a consequence of thermal shock. (Note that the term "stress at fracture" is more accurate in decribing the physical phenomenon, since "strength" is an inherent material property, and may or may not change during the thermal shock procedure. However, the term "strength" is commonly used in literature for similar measurements, and thereby is also used throughout this text.) The thermal shock procedure consisted of quenching the preheated disk with an air jet. During thermal shock the strength of the disk in biaxial flexure was measured at various quenching times (duration of shock), and surface heat transfer coefficients (severity of shock).

Apparatus

The apparatus used for measuring the strength loss of the polycrystalline NaCl disk facilitated three separate tasks:

- Heating up of the disk to a certain temperature
- Generating thermal stresses inside the disk by quenching with air jet
- Measuring the strength in biaxial flexure during quenching.

Figure 1 shows the schematic of the apparatus.

Biaxial Loading

The biaxial loading system consisted of a supporting pin assembly, a loading pin, and a compression tester. The NaCl disk rested on three supporting pins, while the loading pin loaded the disk from the top. The supporting pins were made of carbon steel, 0.32 cm in diameter, with hemispherical tips. These pins were spaced symmetrically on a support circle of 2.0 cm in diameter, and concentric with the loading pin and the test specimen. The loading pin was made of carbon steel, 0.32 cm in diameter, with a flat tip. It was fixed on a stainless steel plate. The compression tester was a Comten model 924 MTC 40/04, 900 series, electric motor driven tester, and was equipped with a digital indicator and a recorder. The compression of the specimen was carried out in a cage with a movable bottom and a fixed top plate. The supporting pin assembly rested on the bottom plate, and the loading pin was mounted on the top plate.

Heating

The heating system consisted of a hot plate, thermocouples, and a temperature indicator. The hot plate had a circular cross section with a central hole through which the loading pin could move. The surface of the hot plate was in direct contact with the specimen disk. A thermally insulating hard brick was attached to the top plate of the compression tester to avoid direct contact between the cage and the hot plate at the time of loading. The disk was insulated around the periphery with ceramic wool.

Air delivery

The air delivery system consisted of a pressurized air supply, plastic tubes, an air filter, flowmeters, glass tubing, and needle valves. The air flow was monitored by Matheson No. 605 rotameters. The inner diameter of the glass tubing which delivered the quenching air was 0.28 cm.

Preparation of samples

Technical grade NaCl was ground in a porcelain mill and was sieved to obtain the fraction of 120-140 mesh. Next, 7.00 g of the material was compacted in a cylindrical die 2.54 cm in diameter with a Carver manual hydraulic laboratory press. The compaction load was 3600 kg. The disk shaped specimens were sintered at 550°C for 6 hours. The heating and cooling were carried out at a rate of 5°C /min to avoid any thermal shock effect. The disks were 2.54 cm in diameter, and 0.78 cm thick after sintering.

Procedure

The specimen disk was placed on the supporting pins and insulated around the periphery with ceramic wool. After the surface temperature of the hot plate had reached 450°C, it was kept constant for 10 min, for a steady temperature distribution inside the disk. The air at ambient temperature (23°C-25°C) was blown onto the disk surface at a flow rate of 0-54 L/min, for 0-180 s. The disk was loaded at a strain rate of 6 mm/min, until fracture. The loading, and the maximum load reached at fracture were recorded. Since it was only possible to predict the time of fracture within ±3 seconds, quenching time was reported within that range.

The equation derived by Kirstein and Woolley [9] for tensile stress, S, for a circular disk in the center of the surface in tension is:

$$S = -\frac{3P}{4\pi d^2}(X - Y) \qquad (1)$$

where:

$X = (1+\mu)1n(B/C)^2 + [(1-\mu)/2](B/C)^2$
$Y = (1+\mu)[1+n(A/C)^2] + (1-\mu)(A/C)^2$
μ = Poisson's ratio
B = radius of loaded area (loading pin cross sectional area)
A = radius of support circle
C = radius of specimen
P = load
t = thickness of disk

In Eq. 1 the specimen and the support circle (the imaginary circle on which support pins were symmetrically placed) were assumed to be concentric. Also, the load was assumed to be applied uniformly over a circular area of radius B in the center of the upper surface. These assumptions are perfectly in accord with the experimental setup, with A = 2.00 cm, B = 0.32 cm, C = 2.54 cm, and t = 0.78 cm. The Poisson's ratio of NaCl was taken as 0.25.

Measurement of the heat transfer coefficients

The severity of quenching was controlled by adjusting the air flow rate. The heat transfer coefficient between the disk surface and the impinging jet of air was taken as a quantitative measure of the severity of thermal shock, and determined as a function of Reynolds number.

Apparatus

Figure 2 shows the schematic of the apparatus used in the heat transfer coefficient measurement. It was a slightly modified version of the biaxial flexure test apparatus. Two thermocouples were placed into the radially drilled holes, extending to the center of the disk.

Procedure

The polycrystalline NaCl disk was placed on the supporting pins and tightened to a fixed position. It was insulated around the periphery with ceramic wool. After the surface temperature of the hot plate had reached 450°C, it was kept constant for 10 min. The disk was quenched by the air jet, at a constant flow rate, until a steady-state temperature gradient was obtained. The two central temperatures inside the disk were recorded. The procedure was repeated at various air flow rates (including no air flow which corresponds to natural convection).

In the calculation of the heat transfer coefficient, the radial heat transfer in comparison to axial heat transfer was neglected, due to the geometry and the radial insulation. At steady-state, one dimensional (axial) heat transfer equations for the disk geometry were used to derive the heat transfer coefficient, as given in Eq. 2 [10],

$$h = \frac{k_1 k_2 (T_1 - T_2)}{\left[\Delta x_1 k_2 (T_2 - T_a) - \Delta x_2 k_1 (T_1 - T_2)\right]} \qquad (2)$$

where,

h = Heat transfer coefficient between the disk surface and the impinging air jet
T_1 = Temperature indicated by thermocouple 1
T_2 = Temperature indicated by thermocouple 2
T_s = Temperature of the disk surface
T_a = Temperature of the air jet
Δx_1 = Separation between the two thermocouples
Δx_2 = Separation between thermocouple 2 and the disk surface
k_1 = Thermal conductivity of sodium chloride [10] given at the average of T_1, and T_2
k_2 = Thermal conductivity of sodium chloride given at the average of T_2, and T_s.

Eq. 2 gives the heat transfer coefficient in terms of the measured values T_1, T_2, Δx_1, and Δx_2. However, in this equation k_2 is

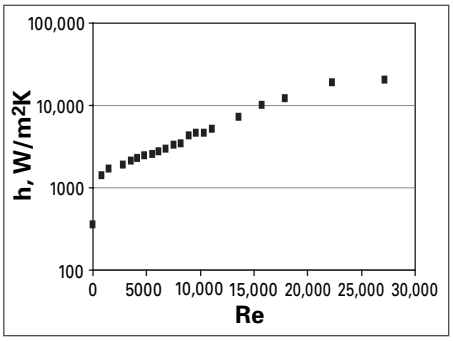

3. Experimentally determined heat transfer coefficient of the impinging air jet as a function of Reynolds number. (T_{air} = 298 K, ρ_{air} = 1.205•10^{-3} g/cm^3,μ_{air} = 1.813•10^{-4} g/cm s, $d_{air\ duct}$ = 0.28 cm).

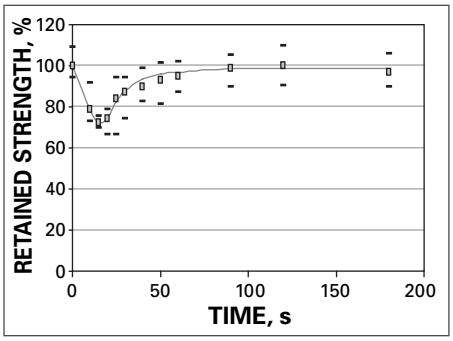

4. Retained strength versus quenching duration for h = 1.7•10^3 W/m^{2}K.

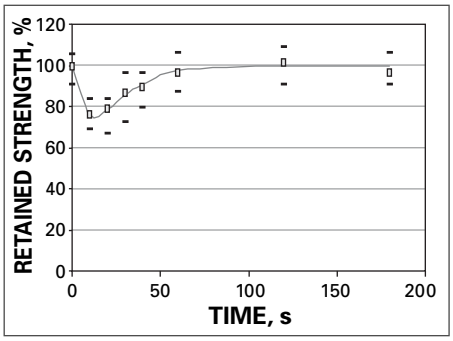

5. Retained strength versus quenching duration for h = 2.1•10^3 W/m^{2}K.

unknown since T_s is not measured. T_s was derived by the same set of heat transfer equations as given in Eq. 3 [10],

$$T_s = T_2 - (T_1 - T_2)\left(\frac{k_1}{k_2}\right)\left(\frac{\Delta x_2}{\Delta x_1}\right) \qquad (3)$$

The unknowns (k_2, and T_s) were calculated by an iterative method using Eq. 3 [10].

RESULTS AND DISCUSSION

The effectiveness of thermal shock in mechanical weakening of the NaCl disks was examined by evaluating the thermal stresses generated by transient temperature gradients. The change in biaxial flexure strength of the preheated specimens during air jet quenching was measured at various durations and severities. The quenching severity was quantified by the value of the heat transfer coefficient of the impinging air jet, while the heat transfer coefficient was determined as a function of Reynolds number.

Determination of the heat transfer coefficient

The heat transfer coefficient of the air jet impinging on the specimen disk was determined on the basis of the steady-state axial heat transfer in the polycrystalline NaCl disk. The surface temperature of the disk was calculated at various air flow rates by the iterative method using Eq. 3. Having determined the disk surface temperatures, the heat transfer coefficients were calculated by Eq. 2, as a function of Reynolds number. **Figure 3** shows the results. The heat transfer coefficients were used as a measure of quenching severity.

Evaluation of thermal stresses by biaxial flexure test

As noted, $\sigma_f/E\alpha$ and k are the parameters that govern thermal shock resistance of materials. Martinez [3] determined the linear expansion coefficient, α, of superheater deposits to be approximately of the same magnitude as single crystal NaCl, numerically 5.2•10^{-5}m/mK. For practical purposes theoretical fracture strength of solids is usually taken as 1/15th of elastic modulus [11]. Therefore, the ratio σ_f/E is expected to be of the same magnitude for the deposit and NaCl. Ozcan [10] experimentally determined the thermal conductivity, k, of polycrystalline NaCl and superheater deposits to be around 1.8 W/m K at 900 K. Therefore, it is justifiable to use NaCl as representative of the deposit in thermal shock tests because of the comparable values of the parameters that determine thermal shock resistance.

The thermal shock was achieved by air jet quenching of the preheated disk. Duration of quenching (time) and the severity of quenching (heat transfer coefficient) were the parameters examined. The mechanical weakening was quantified by measuring the strength of the disk in biaxial flexure, and reported as the percentage of the original unquenched strength. **Figures 4–9** show the results.

Single classification analysis was used to analyze a data subset within a group, and the group means were compared by t-test [10]. It showed that the probability of the differences between the means in a group to arise from indeterminate errors was less than 0.1%. Therefore, it was concluded that the patterns in Figs. 4–9 illustrated determinate effects that were different from statistical fluctuations.

Because the material used in the tests was polycrystalline, it theoretically contained flaws before quenching, especially, in the grain boundaries. The thermal stresses generated during quenching could have damaged the material in a few possible ways, as described in the introduction. Spalling was not observed; hence the damage was expected to be in the form of either propagation of pre-existing cracks, or generation of additional stresses during loading.

Figure 4 shows the retained strength (reported as percent of the unquenched strength) versus time plotted for h = 1.7•10^3 W/m^{2}K. This heat transfer coefficient corresponds to the lowest flow rate used for quenching (Re = 1.5•10^3). The retained strength decreased steeply, and reached a minimum in a relatively short time. It tended to increase to the original strength value as time elapsed. The strength eventually reached the original value, suggesting that there was no change in the inherent strength related properties of the material. The thermal shock was not severe enough for crack propagation. Nevertheless, the strength decreased to 72% of the original at around 15–20 s. The surface was in tension during quenching, and biaxial flexure loading also generated tensile stresses on the disk surface. Therefore, the thermal stresses constituted additional stresses during loading, causing the disk to fail at a lower biaxial flexure load. The retained strength should have reached the minimum at the point when the transient thermal stress reached its maximum, and then gradually returned to the original value. This phenomenon is consistent with the theory that during quenching, thermal stress at the surface

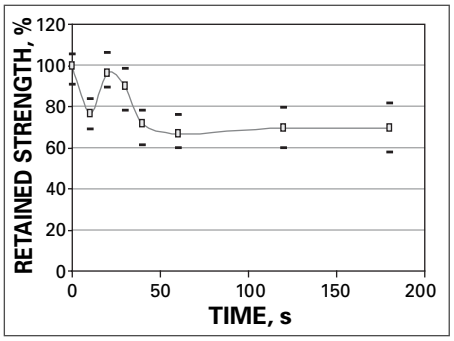

6. Retained strength versus quenching duration for h = 3.3•10³ W/m²K.

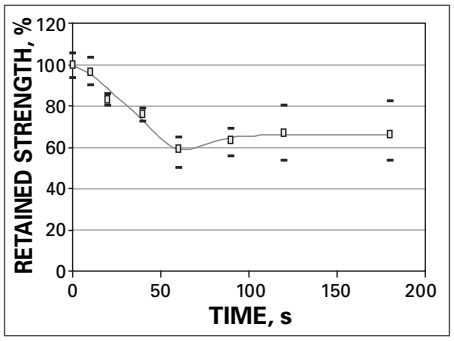

7. Retained strength versus quenching duration for h = 4.9•10³ W/m²K.

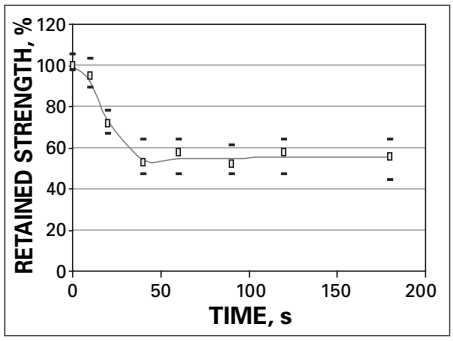

8. Retained strength versus quenching duration for h = 12.2•10³ W/m²K.

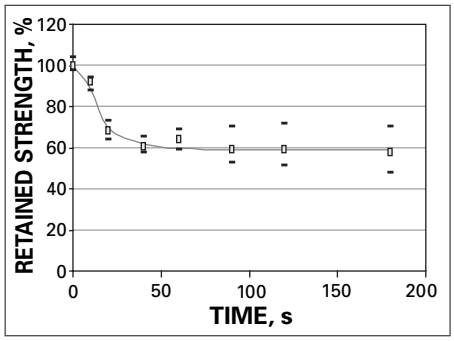

9. Retained strength versus quenching duration for h = 20.1•10³ W/m²K.

reaches a maximum, after which it diminishes with time as the temperature gradient approaches its steady-state value.

The maximum risk of rupture criterion for failure can be used for a more accurate assessment of the result. For a thermally shocked body, the risk of rupture passes through a maximum, after which it gradually diminishes (provided that there is no change in inherent strength-related properties of the material). When the risk of rupture increases, the body becomes more vulnerable to outside loading that would constitute additional stresses to the thermal stresses. At the time of maximum risk of rupture, the resistance to fracture by outside loading is expected to be lowest, rendering the measured strength a minimum. The conclusion from examining Fig. 4 in the light of the maximum risk of rupture criterion is that the observed trend of strength versus time curve was due to transient thermal stresses.

A possible explanation of the phenomenon in microscale can be the formation of microcracks in the grain boundaries on the surface. Tensile thermal stresses would tend to open up the grains to form cleavage cracks. As the thermal stresses diminish, the cleavages close, which can be thought of as microcrack healing. When a cleavage is induced on the surface, stresses amplify in the region around its tips, and if that reaches a certain magnitude, the cracks start to propagate.

In Fig. 5 the retained strength is plotted as a function of time for h = $2.1 \cdot 10^3$ W/m²K. Although the quenching severity was increased, the trend is similar to the case in Fig. 4. The retained strength dropped to a minimum value of approximately 75% of the original at about 10–15 s. The thermal stresses at the surface reached a higher value in a shorter time, with an increase in quenching severity (a larger heat transfer rate). This, in turn, caused the retained strength to reach its minimum in a shorter time (approximately 5 s shorter). The general trend of the curve can be interpreted in much the same way as for the curve illustrated in Fig. 4.

When the quenching severity was increased to h = $3.3 \cdot 10^3$ W/m²K, the general trend of the retained strength versus time curve changed (Fig. 6). The effects of the transient thermal stress were still observed, which resulted in a minimum of approximately 77% of the original strength at about 10 s. The retained strength started to decrease again at around 20 s, and having reached a lowest value of approximately 68% of the original at about 60 s, it remained virtually constant for later times. At this quenching severity, the thermal stresses apparently affected the inherent strength related properties of the material due to surface crack propagation. As described previously, when the quenching severity exceeds a critical limit, cracks start to propagate and rapidly reach their subcritical value, with a corresponding abrupt decrease in material strength. The crack length does not change unless the thermal stress is increased above a second critical limit. Because the severity of shock was kept constant in the test, the strength did not decrease any further.

Figures 7–9 illustrate the retained strength versus time curves at higher heat transfer coefficients. These curves do not show transient minima in strength, which could be attributed to the occurrence of these minima at very short times beyond the detection limits of the setup. This hypothesis is supported by the fact that the thermal stress at the surface reached its maximum at a shorter time with increasing heat transfer coefficient. In Fig. 7, the retained strength reached the lowest value of approximately 60% in about 60 s and remained constant thereafter. When the heat transfer coefficient was $4.9 \cdot 10^3$ W/m²K, the short cracks propagated and reached their final upper limit at approximately 60 s by an accompanying decrease in strength. The severity of shock was not sufficient for the crack propagation to restart in a quasi-static manner.

For the curves in Figs. 8 and 9, with heat transfer rates of $12.2 \cdot 10^3$ W/m²K and $20.1 \cdot 10^3$ W/m²K, the strength reached the lowest value of approximately 57% in about 40 s, and remained virtually constant at later times. The decrease in strength was due to irreversible material damage that could have been attributed to kinetic crack propagation up to its upper limit of stability at about 40 s. However, the severity of shock was not again sufficient for quasi-static crack propagation. Although in Fig. 9 the strength showed a relatively slight

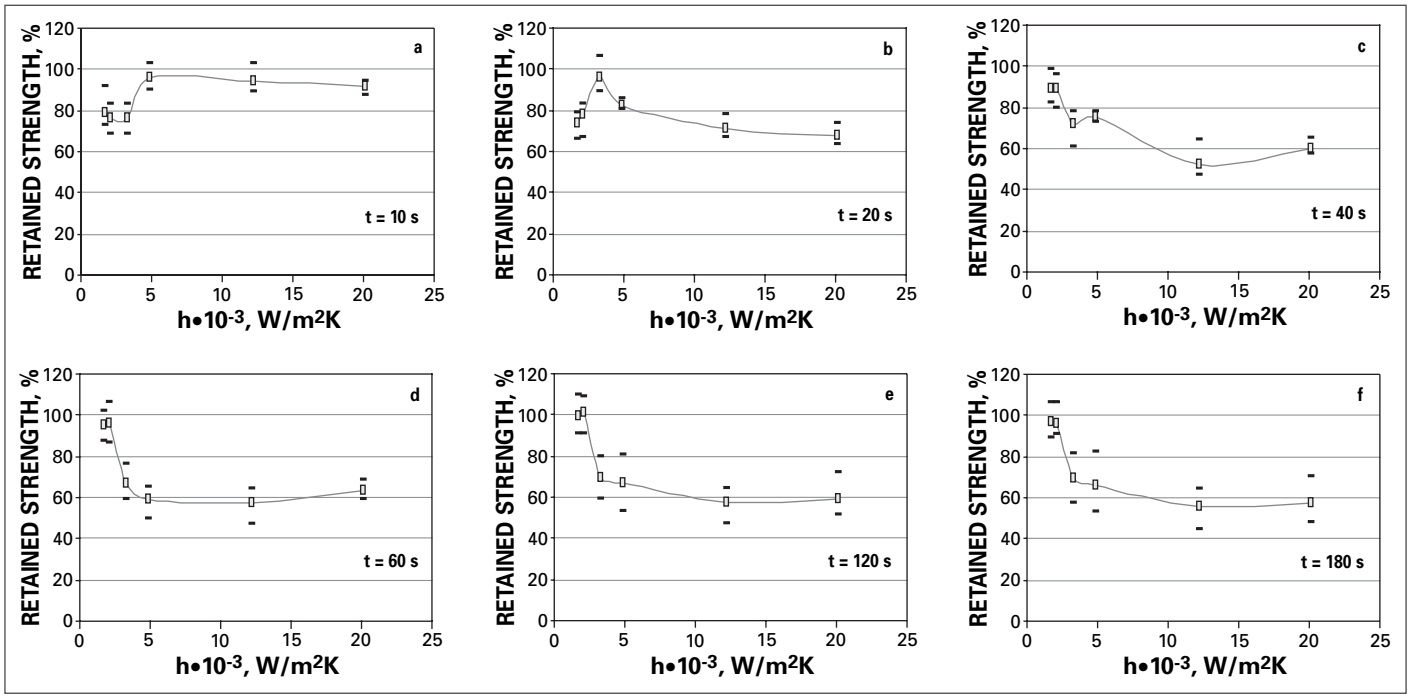

10 (a–f). Retained strength versus heat transfer coefficient for various quenching durations.

decrease with time, it was not possible to attribute this to continuing quasi-static crack propagation because of statistical fluctuations. Nevertheless, comparison of the curves in Figs. 6–9 showed that the time elapsed for the cracks to reach their upper limit of stability did not change by increasing heat transfer rate, which was around 40 s.

Figure 10 illustrates the retained strength versus heat transfer coefficient of the quenching air jet for various quenching durations. At t = 10 s (Fig. 10 a), the lowest time value depicted, retained strength was constant at 77% of the original up to a heat transfer coefficient of about $3.3 \cdot 10^3$ W/m²K, after which it rose steeply to a value of 97% and remained constant for higher values. This result showed that at t = 10 s, the crack propagation did not start and the transient stresses disappeared faster with the increasing heat transfer coefficient.

At a later time, t = 20 s (Fig. 10 b), the effect of transient stresses was still recognizable. Although the retained strength did not decrease permanently at heat transfer coefficient values below $3.3 \cdot 10^3$ W/m²K, the effect of crack propagation with accompanying permanent material damage was seen at higher heat transfer rates. At times t ≥ 40 s (Figs. 10c–f), transient thermal stress effect virtually disappeared and the retained strength returned to its original value at heat transfer coefficients below $3.3 \cdot 10^3$ W/m²K. At higher heat transfer rates, however, the cracks reached their final upper limit of stability at t = 40 s for heat transfer coefficients over $12.2 \cdot 10^3$ W/m²K, and at t ≥ 60 s for heat transfer coefficients over $4.9 \cdot 10^3$ W/m²K. Again these figures provided evidence that quasi-static crack propagation did not take place above the upper crack length limit.

These results are consistent with theoretical considerations. Final crack length depends on the initial crack length (inherent material property) and the severity of quenching. If the quenching severity is below a certain critical limit, cracks do not propagate (Figs. 4 and 5). In addition, the final crack length does not change with quenching severity until it reaches a second critical limit (Figs. 6–9). Therefore, it can be deduced that at a given quenching severity that is high enough for crack propagation, strength would decrease to a constant lower value in a period of time, and once the cracks have reached their final length, strength does not change further. Increasing the quenching severity within a certain limit would affect neither the final crack length nor the final strength, as consistent with the observations. However, increasing the quenching severity beyond a second critical limit causes the crack length to increase in a quasi-static manner, which was not observed.

The biaxial flexure test data can be used to show the existence of a region of quenching severity and duration for an effective mechanical weakening in the deposits. The 35%–40% permanent reduction in the biaxial flexure strength was achieved at heat transfer coefficients above $3.3 \cdot 10^3$ W/m²K, and at quenching durations above 40 s. This defines a maximum thermal shock effect region of quenching time-quenching severity.

CONCLUSIONS

The existence of thermal stresses within a material was shown by strength measurements during thermal shock. It was observed that thermal shock weakens deposit-like materials by causing transient thermal stresses (reversible effect) and crack propagation (irreversible effect damaging the material permanently) simultaneously. Time (duration of quenching) was introduced as a parameter in strength versus quenching severity measurements. Transient thermal stresses caused the biaxial flexure strength of NaCl pellets to be reduced by 25% for

quenching durations less than 20 s, which was observed as minima in the strength versus heat transfer coefficient curves. The propagation of pre-existing cracks during the air-jet quenching permanently reduced the biaxial flexure strength of the material by 35%–40% at heat transfer coefficients above $3.3 \cdot 10^{-3}$ W/m^2K. The time interval for the pre-existing cracks to reach their final length was roughly 40 s for polycrystalline NaCl, and was found to be independent of the quenching severity. These constitute the boundaries of the region that can provide the maximum thermal shock effect. If the quenching severity or the quenching duration is above these limits the maximum thermal shock effect is achieved. The sootblowing process is most beneficial for the cleaning of fireside deposits if the duration and severity of quenching fall in the maximum thermal shock effect region. **TJ**

LITERATURE CITED

1. Tran, H.N., *Kraft Recovery Boilers - Chapter 9: Upper Furnace Deposition and Plugging*, edited by T.N. Adams, TAPPI Press, p. 245-282 (1997).
2. Shenassa, R., Kuhn, D.C.S. Kuhn, and H.N. Tran, *Journal of Pulp & Paper Canada*, 29(4): 132(2003).
3. Martinez, M., "Enhanced removal of kraft recovery boiler fireside deposits by thermal shock," MASc thesis, Chemical Engineering, University of Toronto, 1990.
4. Boley, B.A. and Weiner, J.H., *Theory of Thermal Stresses*, John Wiley and Sons, New York, 1960.
5. Manson, S.S. and Smith, R.V., "Quantitative evaluation of thermal shock resistance," American Society of Mechanical Engineers, preprint No. 54-A-263, 533-544 (1954).
6. Manson, S.S. and Smith, R.V., *J. Amer. Ceram. Soc.* 38(1): 18(1955).
7. Goodrich, H.R., *J. Amer. Ceram. Soc.* 10(10): 784(1927).
8. Hasselman, D.H., *J. Amer. Ceram. Soc.* 52(11): 600(1969).
9. Kirstein, A.F. and Wooley, R.M., *J. Research*, National Bureau of Standards, JNBAA, 71C, 1-10 (1967).
10. Ozcan, S., "Recovery boiler fireside deposit thermal shock resistance and thermal conductivity," MASc thesis, Chemical Engineering, University of Toronto, 1991.
11. Piggott, M.R., *Load Bearing Fibre Composites*, Pergamon Press, New York, 1981.

Received: January 31, 2006
Revised: February 28, 2006
Accepted: March 1, 2006

This paper is also published on TAPPI's web site <www.tappi.org> and summarized in the April *Solutions! for People, Processes and Paper* magazine (Vol. 89 No. 4).

INSIGHTS FROM THE AUTHORS

Fireside deposit plugging of the kraft recovery boilers in the pulp and paper industry is a formidable problem. It can be addressed more efficiently by mastering the underlying scientific principles, especially in terms of the thermal shock resistance of the deposit materials, and the thermal stresses generated during the "chill-and-blow" procedure.

This research complements graduate research conducted by M. Martinez on enhanced removal of kraft recovery boiler fireside deposits by thermal shock. It brings about new scientific explanations of the nature of the thermal stresses that develop during the thermal shock procedure.

The design of the experimental setup to quantify the mechanical weakening effect of the thermal stresses that develop during the thermal shock of the deposit-like materials was the most difficult aspect of this research. Measurements showed a statistical distribution that was addressed by a comprehensive statistical analysis for the evaluation of the results.

The limits in terms of quenching severity and quenching duration for a more efficient cleaning of the fireside deposits were quantified. It was especially interesting to observe the mechanical weakening effect of the transient thermal stresses as well as the crack propagation.

If the quenching severity or the quenching duration is above the limits described in the article, the maximum thermal shock effect is achieved. The sootblowing process is most beneficial for the cleaning of fireside deposits if the duration and severity of quenching fall in the maximum thermal shock effect region.

The next steps could be the investigation of the effectiveness of the interfacial thermal stresses in deposit cleaning, as well as inclusion of certain materials in black liquor to decrease the thermal shock resistance of the deposit materials, and to decrease the stickiness of the deposit material on carbon steel.

— Selcuk Özcan

Özcan

Özcan is a Ph.D. candidate in the Department of Chemical Engineering, Izmir Institute of Technology, Urla, Izmir, Turkey; Tran is with the Department of Chemical Engineering and Applied Chemistry, University of Toronto, Toronto, Ontario, Canada. Email Özcan at thtinc@yahoo.com or selcukozcan@iyte.edu.tr. Email Tran at tranhn@chem-eng.utoronto.ca.

Tran